Journal of Metals, Materials and Minerals, Vol. 32, No. 2, pp. 70-76, 2022

Brazilein modified zinc oxide nanorods with enhanced visible light-responsive photocatalytic efficiency

Montri AIEMPANAKIT[1], Penpicha SUDJAI[2], Kittiyaporn SINGSUMPHAN[1], Sakchai LAKSEE[3], and Cheewita SUWANCHAWALIT[2,*]

[1] *Department of Physics, Faculty of Science, Silpakorn University, Nakhon Pathom, 73000, Thailand*
[2] *Department of Chemistry, Faculty of Science, Silpakorn University, Nakhon Pathom, 73000, Thailand*
[3] *Nuclear Technology Research and Development Center, Thailand Institute of Nuclear Technology (Public Organization), Nakhon Nayok, 26120, Thailand*

***Corresponding author e-mail:** suwanchawalit_c@su.ac.th

Received date:
6 March 2022
Revised date
16 April 2022
Accepted date:
28 April 2022

Keywords:
ZnO;
Brazilein modified ZnO;
Impregnation method;
Visible light-responsive photocatalyst;
Degradation of indigo carmine

Abstract

Photocatalytic efficiency of ZnO nanorods has been investigated with respect to the concentration of brazilein. Brazilein modified ZnO nanorods were prepared by an impregnation process with 1.0%w/v, 2.5%w/v, and 5.0%w/v of brazilein solution. In order to correlate the variation in concentration distributions and photocatalytic performance, the phase composition, optical properties, and photocatalytic activities of brazilein modified ZnO nanorods prepared with different brazilein concentrations have been investigated and compared to an unmodified ZnO nanorods. The photocatalytic properties were measured in terms of indigo carmine degradation under visible light irradiation. It was found that ZnO nanorods with the highest visible light-responsive photocatalytic efficiency were achieved by the modification of 5.0%w/v of brazilein resulting in indigo carmine degraded faster than the case of unmodified ZnO nanorod about 60% within 5 h.

1. Introduction

Alternative methods for the removal of pollutants, such as heterogeneous photocatalysis based on semiconductor catalysts, have garnered a lot of interest [1-3]. Zinc oxide (ZnO) has recently gained a lot of attention as a promising photocatalytic material for removing organic contaminants from wastewater, owing to its high catalytic activity, low preparation cost, and ecologically friendly nature [4,5]. ZnO is an n-type semiconductor with a 3.37 eV wide bandgap and a high excitation binding energy of 60 meV. However, the application of pure ZnO in photocatalysis under visible and solar light is restricted due to its wide band gap and quick recombination of electron-hole pairs [6,7]. To solve these drawbacks, many researchers developed various methods, such as metal and nonmetal doping [8-11], coupling with other narrow-band gap semiconductors [12-14] and dye-sensitized semiconductors [15-20]. The use of dye molecules to sensitize ZnO particles is considered to be an effective way to expand light absorption into the visible region while also improving their photocatalytic activities. Some common dye sensitizers include alizarin red S dye [16], porphyrin [21-23] and natural dyes [17,24].

Brazilein is a common natural red dye extracted from *Caesalpinia sappan* wood. The chemical structure of brazilein is shown in Figure 1. Brazilein has many useful as photo sensitizer for dye sensitized solar cell [25], color pigment [26], acid base indicator [27], sensor [28], antioxidant and antitumor [29,30]. In the present work, the brazilein was used as a sensitizer of ZnO nanorods photo-catalyst to extend the light absorption in visible region. Brazilein modified ZnO (Bra-ZnO) nanorods photocatalysts were prepared via an impregnation process. The effect of brazilein contents on the microstructural, optical, and photocatalytic properties were evaluated. The photocatalytic activity of the ZnO and Bra-ZnO nanorods was tested by using indigo carmine (IC) as a model organic pollutant. The generated hydroxyl radical (•OH) during the photocatalytic oxidation process was measured, and possible photocatalytic mechanism was also presented.

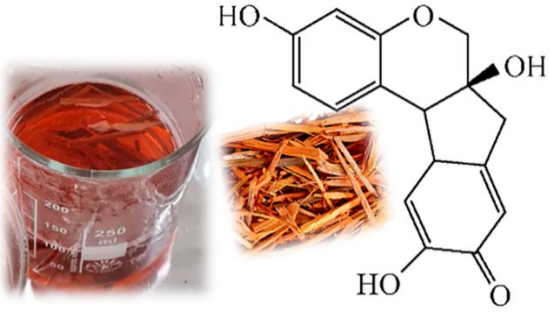

Figure 1. Chemical structure of brazilein extracted from sappan wood.

 DOI: 10.55713/jmmm.v32i2.1255

2. Experimental

2.1 Preparation of ZnO thin films

ZnO thin films were deposited using the direct current magnetron sputtering (DCMS) mode with ZnO sputtering target disk of 75 mm in diameter and 6 mm thick. The sputtering process was performed in a high vacuum chamber with a base pressure below 5×10^{-5} mbar using coupled diffusion and rotary pumps. The FTO glass substrates (1.5 cm × 2.5 cm) were ultrasonically cleaned in acetone and methanol for 15 min and blow-dried with nitrogen gas. The target-substrate distance was kept at 60 mm. Ar (99.9997% purity) flow of 30 sccm was introduced into the chamber to provide a sputtering pressure of 6×10^{-3} mbar, controlled by a mass flow controller. Before ZnO deposition, the target was pre-sputtered for 5 min in order to clean the target surface. The sputtering power was 100 W and the deposition time was 8 min. After deposition, all films were annealed at a temperature of 400°C for 3 h under normal ambient air. These ZnO films were used as the substrate for the hydrothermal process.

2.2 Preparation of ZnO nanorods

ZnO nanorods were prepared by using the hydrothermal method. ZnO thin films deposited FTO glass were used as a seed layer. The hydrothermal autoclave made of high strength stainless steel was used to control the chemical dissolution of the formed ZnO nanorods. For the preparation of a precursor solution, 150 mL of hexamethylene-tetramine (HTMA; $C_6H_{12}N_4$) aqueous solution (25 mM) was mixed with 150 mL of zinc nitrate hexahydrate ($Zn(NO_3)_2.6H_2O$) aqueous solution (25 mM). The mixed solution was stirred at room temperature for 10 min. Then the mixture was transferred into a Teflon lined stainless steel autoclave. The hydrothermal process was heated to 105°C for 5 h in an oven and then cooled down naturally for 10 min. The obtained ZnO nanorods were rinsed with distilled water and dried at 60°C in an oven for 12 h.

2.3 Preparation of brazilein modified ZnO nanorods

Brazilein solution was extracted from sappan wood at 55°C for 5 h using methanol: water (50:50) as the solvent, resulting in the red solution which was then filtered. Different concentrations of brazilein solutions (1.0%w/v, 2.5%w/v, and 5.0%w/v of brazilein) were prepared. Bra-ZnO nanorod was prepared by an impregnation process. Briefly, four pieces of ZnO nanorods films were soaked in 50 mL brazilein solution (1.0%w/v, 2.5%w/v, and 5.0%w/v of brazilein) for 10 h and then denoted as 1.0Bra-ZnO, 2.5Bra-ZnO, and 5.0Bra-ZnO, respectively. The obtained Bra-ZnO nanorods films were rinsed with methanol: water solvent and dried at 60°C in an oven for 12 h as shown in Figure 2.

2.4 Characterizations

The crystal structures of the ZnO and Bra-ZnO nanorods were investigated by X-ray diffraction (XRD) technique (Rigaku MiniFlex II X-Ray diffractometer) using Cu Kα source (λ = 1.5406 Å) with scanning range 2θ from 20° to 70°. The morphology and chemical composition were investigated via a field emission scanning electron microscopy (FE-SEM, TESCAN model MIRA3) and energy-dispersive X-ray spectrometer (EDS). In order to study chemical surface structure, Fourier-transformed infrared (FTIR) spectra were measured by FTIR spectrophotometer (Perkin Elmer Spectrum Bx) in the range of 400 cm^{-1} to 4000 cm^{-1}. The diffuse reflectance absorption spectra were monitored using UV-Visible spectrophotometer (Shimadzu UV2401) for study of the optical properties and band gap energy.

2.5 Measurement of photocatalytic activity

The photocatalytic activity of the ZnO and Bra-ZnO nanorods were evaluated by the photocatalytic degradation of IC under visible light from fluorescent lamp (TL-D 18 W/865 Philips tube light). Four pieces of the ZnO nanorods or Bra-ZnO nanorods were immersed in 50 mL of IC solution (1.0×10^{-5} M) in the dark for 1 h to allow the adsorption/desorption reached balance. Then two 18-W fluorescent lamps without UV filter placed approximately 15 cm from the samples were turned on to boot the photocatalytic activity [31]. While stirring and irradiation, the solution of 2 mL to 3 mL was collected every hour. The remaining concentration of IC was determined by a UV-Visible spectrophotometer.

The photocatalytic efficiencies of the ZnO and Bra-ZnO nanorods were determined in terms of photocatalytic efficiency (%). In order to compare the speeds of the photocatalyst under light irradiation, the apparent rate constants (k) were obtained from slopes of the graphs by plotting ($ln(C_t/C_0)$ versus time. The photocatalytic efficiency (%) and pseudo-first-order rate constants can be calculated using the following equations (1-2):

$$\text{Photocatalytic efficiency (\%)} = \frac{C_0 - C_t}{C_0} \times 100 \qquad (1)$$

$$-ln(C_t/C_0) = kt \qquad (2)$$

Where C_0 and C_t are the initial and remaining concentrations of IC at the different irradiated time (t), respectively.

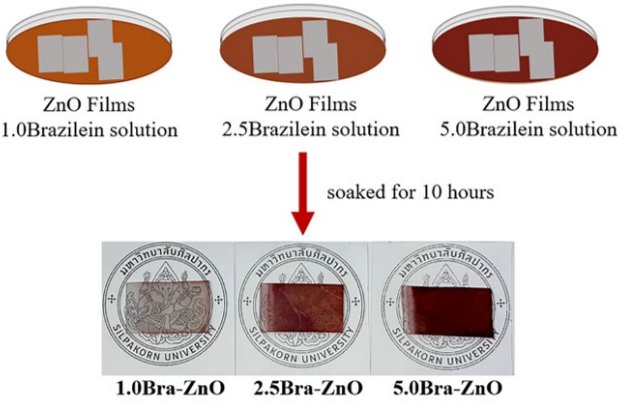

Figure 2. Preparation of the Bra-ZnO nanorods.

2.6 Measurement of hydroxyl radical

Using terephthalic acid as a hydroxyl radical (•OH) scavenger, the formed •OH during the photocatalytic reaction was investigated. The experiment details were similar to the previous work [19,20,32]. The emission peak was at 424 nm under excitation wavelength 315 nm by using fluorescence analysis (Perkin Elmer LS-50B Luminescence Spectrometer).

3. Results and discussion

3.1 Microstructure and optical properties

The morphologies of ZnO and Bra-ZnO nanorods were evaluated by FE-SEM technique as illustrated in Figure 3. It was observed that a needle-like morphology with poorly alignment was the predominant structural feature. There was the variation in diameters of the different nanorods. Nonetheless, the diameter of each nanorod was uniform along its entire length. The average diameter and length of the ZnO nanorods are 50 nm and 1200 nm, respectively. The alignment of the ZnO nanorods and uniform distribution of nanorods diameter could be affected by surface roughness of seed layer. Thus, our case could be caused by the rough ZnO seed layer based on the DCMS method. After impregnation process, it was observed that brazilein adsorbed on the surface of ZnO nanorod. This is clearly seen in the case of high content of brazilein (5.0Bra-ZnO). It should be noted especially that brazilein was generally well-adsorbed throughout their length for each nanorod and the thickness of brazilein also increased with increasing brazilein contents. The elemental composition of ZnO and Bra-ZnO nanorods was investigated by EDS as shown in Table 1. Results confirmed the existence of brazilein on the surface of the ZnO nanorods. It was found that the at% of C element increased with increasing brazilein concentrations.

The XRD patterns of ZnO and Bra-ZnO nanorods at different brazilein concentrations were shown in Figure 4. Our data were in well agreement with the JCPDS PDF no. 77-0452 (SnO_2) and JCPDF PDF no 36- 1451 (ZnO). For FTO glass substrate, the XRD pattern showed multiple diffraction peaks at 2θ angles of 26.5°, 33.7°, 37.7°, 51.9°, 54.6°, 61.6° and 65.7° corresponding to (110), (101), (200), (211), (220), (310) and (301) planes, respectively. The XRD pattern of ZnO showed characteristic peaks with hexagonal wurtzite structure at 2θ of 31.8°, 34.4°, 36.3°, 47.5°, 56.6°, 62.9°, 67.9°, 69.0° corresponding to (100), (002), (101), (102), (110), (103), (112) and (201) planes, respectively. These peaks were clearly seen in ZnO and 1.0Bra-ZnO samples, while the diffraction peak intensities of 2.5Bra-ZnO and 5.0Bra-ZnO decreased possibly due to the high amount of brazilein on the surface of the ZnO nanorods, consistent with the EDS results.

The surface chemical compositions of ZnO and Bra-ZnO nanorods were investigated with FTIR as shown in Figure 5. The FTIR spectra of both ZnO and Bra-ZnO nanorods revealed vibration bands of the Zn-O bond at 400 cm^{-1} to 750 cm^{-1} [33], the broad band of O-H stretching mode of the hydroxyl group at 3000 cm^{-1} to 3600 cm^{-1} [19,33], and O-H bending mode of the hydroxyl group at 1640 cm^{-1} [19,33]. The results also showed the existence of brazilein molecules on the surface of the Bra-ZnO nanorods, with intensities of C=O at 1415 cm^{-1} and C=C bands at 1595 cm^{-1} and C–H band in the aromatic ring within the wavenumber range of 650 cm^{-1} to 860 cm^{-1} and aliphatic C-H band at around 2871 cm^{-1} to 2925 cm^{-1} were also observed [34-36]. Therefore, the interaction of brazilein molecules and ZnO nanorods surface occurred via hydrogen bonding.

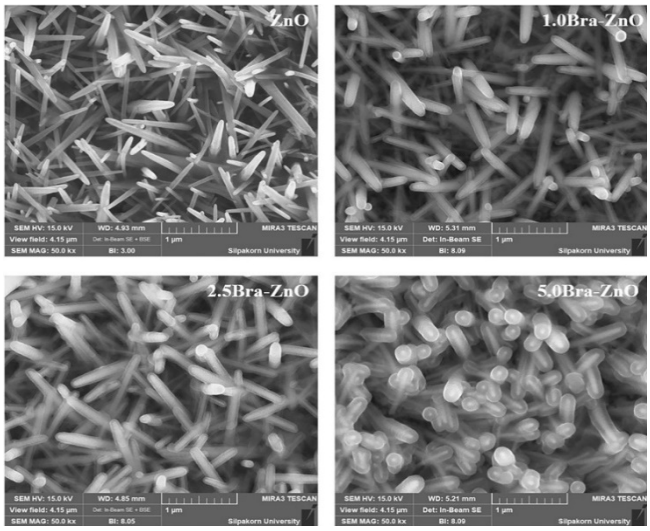

Figure 3. FE-SEM images of ZnO, 1.0Bra-ZnO, 2.5Bra-ZnO and 5.0Bra-ZnO nanorods.

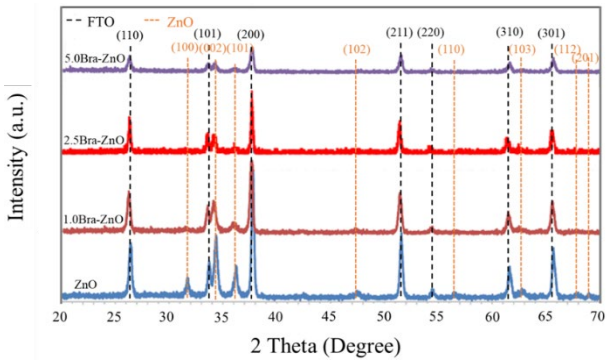

Figure 4. XRD patterns of ZnO and Bra-ZnO nanorods over the 2θ range of 20° to 70°.

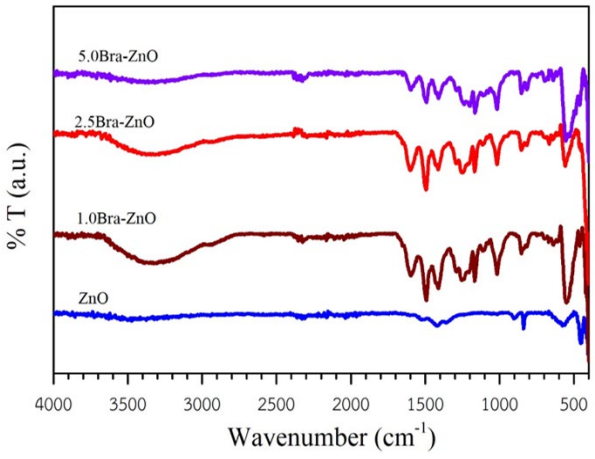

Figure 5. FTIR spectra of ZnO and Bra-ZnO nanorods.

Table 1. Elemental composition of ZnO and Bra-ZnO nanorods.

Samples	Elemental composition (at%)			
	Zn	O	Sn	C
ZnO	28.33	53.69	9.58	8.40
1.0Bra-ZnO	29.84	36.61	3.49	30.06
2.5Bra-ZnO	18.61	33.26	5.10	43.03
5.0Bra-ZnO	10.74	22.06	1.69	65.51

Table 2. The calculated bandgap energy of ZnO and Bra-ZnO nanorods.

Samples	Absorption band edge (nm)	Band gap energy (eV)
ZnO	380	3.26
1.0Bra-ZnO	385	3.22
2.5Bra-ZnO	392	3.16
5.0Bra-ZnO	390	3.18

Figure 6 shows UV-Visible absorption spectra of the ZnO and Bra-ZnO nanorods. It was clear that the Bra-ZnO nanorods exhibited absorption in the UV and visible light region while the ZnO absorbed only UV region. Moreover, the red shift of the Bra-ZnO spectra should enhance photocatalytic efficiency under visible light source. The calculated band gap energy of the Bra-ZnO nanorods decreased when compared with ZnO nanorods as shown in Table 2. The absorption band edge is obtained by the linear extrapolation of the steep part of the UV adsorption toward the baseline [31]. The absorption band edges of each sample were added in Table 2. The band gap energy is calculated from this equation:

$$E_g = h \cdot \frac{c}{\lambda} \quad (3)$$

where E_g is the band gap energy (eV), h is the Planck's constant, c is the light velocity ($m \cdot s^{-1}$), and λ is the wavelength (nm).

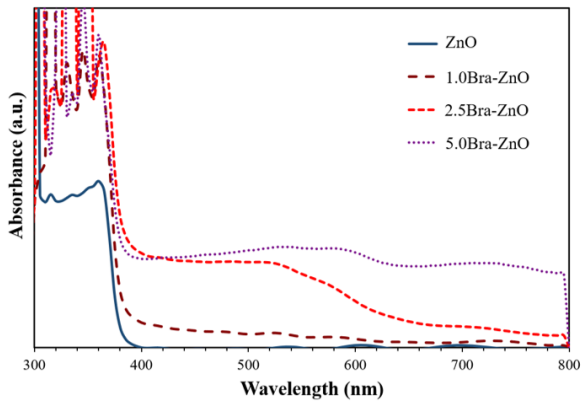

Figure 6. Absorbance spectra of ZnO and Bra-ZnO nanorods.

3.2 Photocatalytic activity

The photocatalytic properties of ZnO and Bra-ZnO nanorods were evaluated by monitoring the degradation of IC under visible light irradiation. The photodegradation efficiency and kinetic results were shown in Figure 7. Several parameters influenced the photocatalytic activity of catalysts, including light absorption, size, shape, surface area, morphological features, and dimensionality [37]. Normally, photocatalytic decolorization involved two processes: pollutant molecule adsorption on the catalyst and photocatalytic decolorization [1,2,38]. The adsorption of IC measured in the dark of ZnO and Bra-ZnO nanorods were approximately 10% and 15% to 20%, respectively. The interaction between ZnO nanorods and IC molecules is hydrogen bonding. For Bra-ZnO nanorods surfaces and IC molecules are more hydrogen bonding and π-π interations. The Bra-ZnO nanorods surfaces exhibited higher interaction than ZnO, giving high percentage of adsorption. The highest activity was observed in the 5.0Bra-ZnO nanorods indicating that the modification of brazilein molecules onto the ZnO surface significantly enhanced the photocatalytic activity. These photocatalytic results revealed that the higher loading of brazilein provide higher photocatalytic activity. Furthermore, high loading of brazilein showed extended absorption in visible region.

The corresponding pseudo-first-order kinetic plots were shown in Figure 7(b). The photocatalytic degradation rate constant (k) of ZnO and Bra-ZnO nanorods were presented in Table 3. The rate constants of 0.157, 0.171, 0.214, and 0.251 h^{-1} were observed in ZnO, 1.0Bra-ZnO, 2.5Bra-ZnO, 5.0Bra-ZnO nanorods, respectively. The R^2 of the kinetic studied were also showed in Table 3. Therefore, rate constant of 5.0Bra-ZnO was 60% greater than rate constant of ZnO.

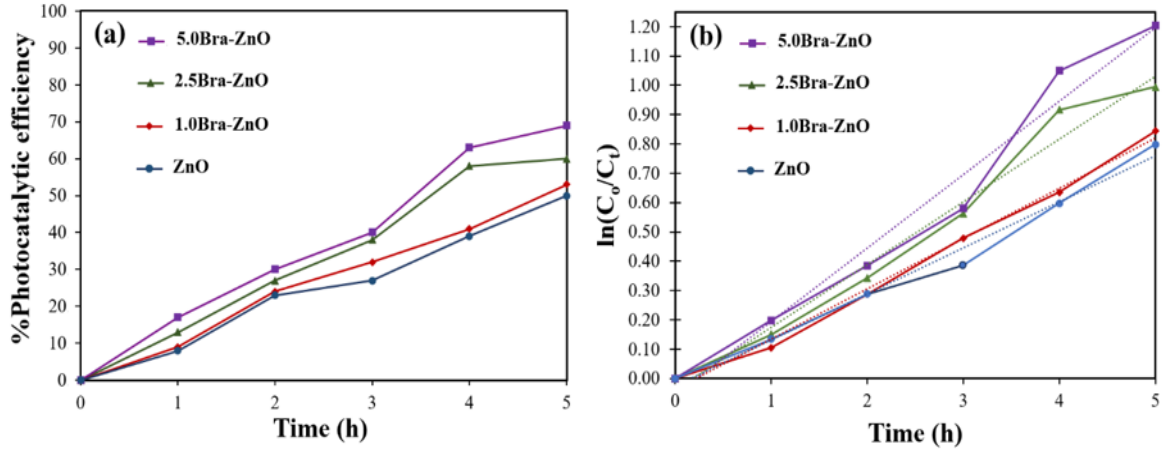

Figure 7. (a) Photodegradation efficiencies and (b) pseudo-first-order kinetic plots of ZnO and Bra-ZnO nanorods under visible light irradiation.

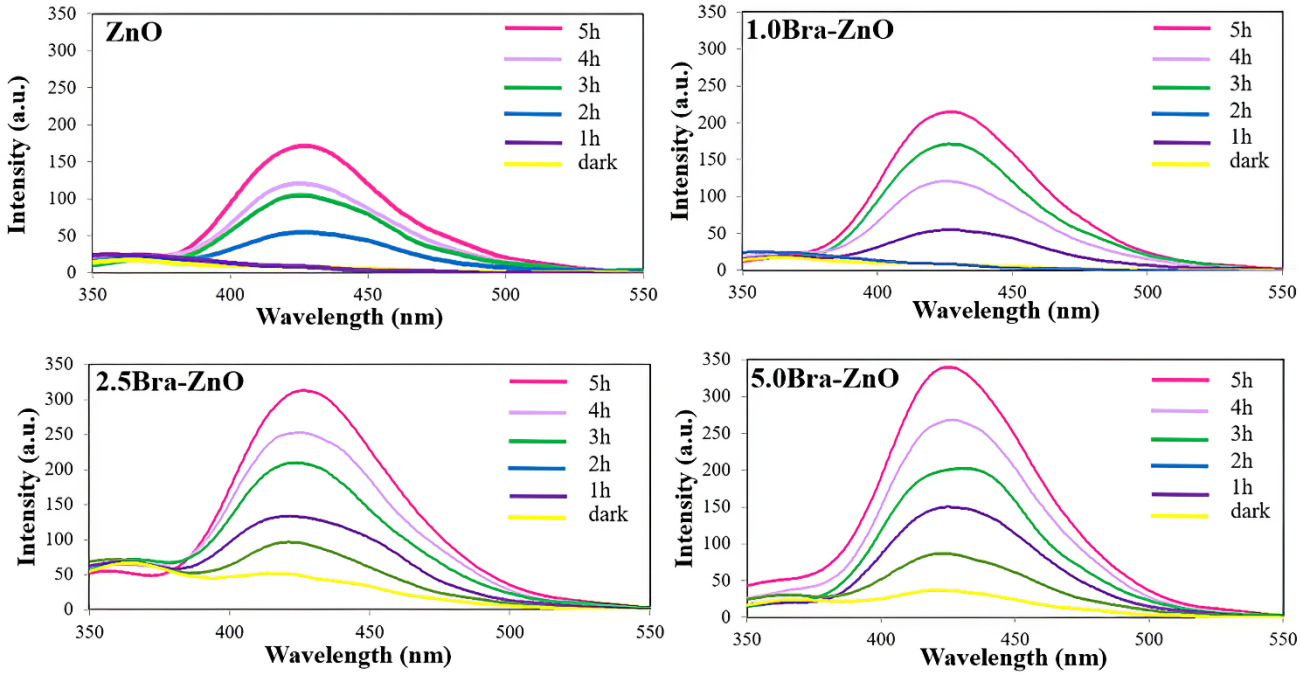

Figure 8. Amount of generated •OH radicals using ZnO and Bra-ZnO nanorods under visible light irradiation.

Table 3. The calculated rate constant of ZnO and Bra-ZnO nanorods.

Samples	Rate constant (k,h^{-1})	R^2
ZnO	0.157	0.9867
1.0Bra-ZnO	0.171	0.9936
2.5Bra-ZnO	0.214	0.9971
5.0Bra-ZnO	0.251	0.9726

The amount of •OH generated by ZnO and Bra-ZnO nanorods under visible light irradiation is represented in Figure 8. The generated •OH increased with increasing irradiation time that corresponded to the high photocatalytic efficiency. From these results, the 5.0Bra-ZnO nanorods produced the highest amount of the •OH generated during photocatalytic process, corresponding with the highest rate constant.

The photocatalyzed reaction of Bra-ZnO nanorods involves the generation of electron-hole pairs via light illumination. Due to the dye molecules' narrower band gap energy, the addition of a dye-sensitizer extends light absorption in visible region. The photoexcited electrons of adsorbed dyes are then injected into the conduction band (CB) of the ZnO photocatalyst. Hydroxyl radicals (•OH) are formed on the surface of Bra-ZnO nanorods and then react with IC, resulting in degradation. A possible photocatalytic mechanism of Bra-ZnO nanorods is shown in Figure 9. The electrons in the brazilein molecule are excited when it is irradiated with visible light, and brazilein can operate as an effective electron donor. The photo-excited electrons are injected into the CB of ZnO. These electrons ($e_{CB}^{\bullet-}$ (ZnO)) subsequently reduce the O_2 adsorbed on the ZnO surface to produce superoxide anion, $O_2^{\bullet-}$ which further convert into H_2O_2 and eventually •OH [39,40]. Because •OH is a powerful and reactive oxidant, it reacts with IC molecules and destroys them. Under visible light irradiation, positively charged brazilein (brazilein$^+$) may interact with surrounding solvent molecules (S) and return to the neutral stage, ready for the next round of excitation [24,41-43]. The proposed mechanism is described by the following equations in Equation (4)-(10):

$$\text{brazilein} + h\nu \rightarrow \text{brazilein}^* \quad (4)$$

$$\text{brazilein}^* + \text{ZnO} \rightarrow \text{brazilein}^+ + e_{CB}^{\bullet-}(\text{ZnO}) \quad (5)$$

$$O_2(\text{ads}) + e_{CB}^{\bullet-}(\text{ZnO}) \rightarrow O_2^{\bullet-} \quad (6)$$

$$O_2^{\bullet-} + H^+ \rightarrow HO_2^{\bullet} \quad (7)$$

$$2HO_2^{\bullet} + H_2O \rightarrow 2H_2O_2 + {}^{\bullet}OH \quad (8)$$

$$\text{IC} + {}^{\bullet}OH \rightarrow \text{degradation products} \quad (9)$$

$$\text{brazilein}^+ + S \rightarrow \text{brazilein} + S^+ \quad (10)$$

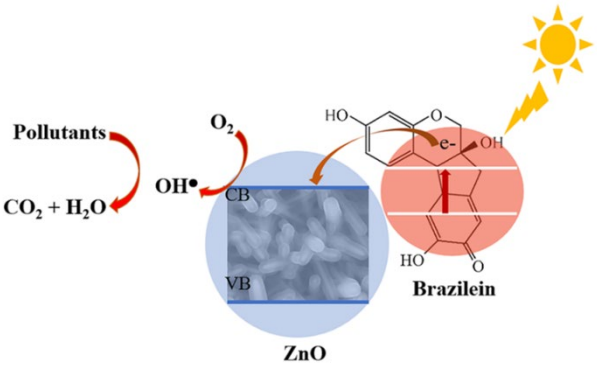

Figure 9. Proposed photocatalytic mechanism of Bra-ZnO nanorods under visible light irradiation.

4. Conclusions

The morphology of ZnO and Bra-ZnO nanorods was needle-like nanostructure. Brazilein was well-adsorbed along the length of each ZnO nanorod. For optical properties, ZnO nanorods exhibited an absorption in the UV region. While Bra-ZnO nanorods illustrated an absorption in both UV and visible light region. The band gap energy of Bra-ZnO nanorods was narrower than that of ZnO nanorods. The results revealed that the highest photocatalytic activity was occurred in 5.0Bra-ZnO. In summary, the higher concentration of brazilein presented the higher photocatalytic activity. Accordingly, Bra-ZnO nanorods could be a good candidate material with natural dye extract for visible light-responsive photocatalytic activity.

Acknowledgements

The author would like to thank the Faculty of Science, Silpakorn University, Nakhon Pathom, Thailand for financial support (Grant No. SRIF-JRG-2563-15).

References

[1] M. R. Hoffmann, S. T. Martin, W. Choi, and D. W. Bahnemann, "Environmenta applications of semiconductor photocatalysis," *Chemical Reviews*, vol. 95, pp. 69-96, 1995.

[2] J. M. Herrmann, "Heterogeneous photocatalysis: State of the art and present applications," *Topics in Catalysis*, vol. 34, pp. 49-65, 2005.

[3] S. Ye, Y. Chen, X. Yao, and J. Zhang, "Simultaneous removal of organic pollutants and heavy metals in wastewater by photo-electrocatalysis: A review," *Chemosphere*, vol. 273, p. 128503, 2021.

[4] C. Hariharan, "Photocatalytic degradation *of* organic contaminants in water by ZnO nanoparticles revisited," *Applied Catalysis A General*, vol. 304, pp. 55-61, 2006.

[5] T. Pauporte, and J. Rathousky, "Electrodeposited mesoporous ZnO thin films as efficient photocatalysts for the degradation of dye pollutants," *Journal of Physical Chemistry C,* vol. 111, pp. 7639-7644, 2007.

[6] D. Kong, Y. Zheng, M. Kobielusz, Y. Wang, Z. Bai, W. Macyk, X. Wang, and J. Tang, "Recent advances in visible light-driven water oxidation and reduction in suspension systems," *Materials Today*, vol. 21, pp. 897-924, 2018.

[7] H. Y. Shu, M. C. Chang, and T. H. Tseng, "Solar and visible light illumination on immobilized nano zinc oxide for the degradation and mineralization of orange G in wastewater," *Catalysts*, vol. 7, p. 164, 2017.

[8] H. T. P. Nguyen, T. M. T. Nguyen, C. N. Hoang, T. K. Le, T. Lund, H. K. H. Nguyen, and T.K.X. Huynh, "Characterization and photocatalytic activity of new photocatalysts based on Ag, F-modified ZnO nanoparticles prepared by thermal shock method," *Arabian Journal of Chemistry*, vol. 13, pp. 1837-1847, 2020.

[9] R. Ebrahimi, K. Hossienzadeh, A. Maleki, R. Ghanbari, R. Rezaee, M. Safari, B. Shahmoradi, H. Daraei, A. Jafari, K. Yetilmezsoy, and S. H. Puttaiah, "Effects of doping zinc oxide nanoparticles with transition metals (Ag, Cu, Mn) on photo-catalytic degradation of Direct Blue 15 dye under UV and visible light irradiation," *Journal of Environmental Health Science and Engineering*, vol. 17, pp. 479-492, 2019.

[10] E. Prabakaran, and K. Pillay, "Synthesis of N-doped ZnO nanoparticles with cabbage morphology as a catalyst for the efficient photocatalytic degradation of methylene blue under UV and visible light," *RSC Advances*, vol. 9, pp. 7509-7535, 2019.

[11] S. Thaweesak, S. Wang, M. Lyu, M. Xiao, P. Peerakiatkhajohn, and L. Wang, "Boron-doped graphitic carbon nitride nanosheets for enhanced visible light photocatalytic water splitting," *Dalton Transactions*, vol. 46, pp. 10714-10720, 2017.

[12] K. Xu, Z. Liu, S. Qi, Z. Yin, S. Deng, M. Zhang, and Z. Sun, "Construction of Ag-modified TiO_2/ZnO heterojunction nanotree arrays with superior photocatalytic and photoelectrochemical properties," *RSC Advances*, vol. 10, pp. 34702-34711, 2020.

[13] T. Munawar, F. Iqbal, S. Yasmeen, K. Mahmood, and A. Hussain, "Multi metal oxide NiO-CdO-ZnO nanocomposite–synthesis, structural, optical, electrical properties and enhanced sunlight driven photocatalytic activity," *Ceramics International*, vol. 46, pp. 2421-2437, 2020.

[14] P. Peerakiatkhajohn, T. Butburee, J. -H. Yun, H. Chen, R. M. Richards, and L. Wang, "A hybrid photoelectrode with plasmonic Au@TiO_2 nanoparticles for enhanced photoelectrochemical water splitting," *Journal of Materials Chemistry A*, vol. 3, pp. 20127-20133, 2015.

[15] D. Chatterjee, and S. Dasgupta, "Visible light induced photo-catalytic degradation of organic pollutants," *Journal of Photo-chemistry and Photobiology C: Photochemistry Reviews*, vol. 6, pp. 186-205, 2005.

[16] G. C. C. Yang, and S. -W. Chan, "Photocatalytic reduction of chromium(VI) in aqueous solution using dye-sensitized nanoscale ZnO under visible light irradiation," *Journal of Nanoparticle Research*, vol. 11, pp. 221-230, 2009.

[17] A. Zyoud, M. Dwikat, S. Al-Shakhshir, S. Ateeq, J. Shteiwi, A. Zu'bi, M. H. S. Helal, G. Campet, D. Park, H. Kwon, T. W. Kim, M. Kharoof, R. Shawahna, and H. S. Hilal. "Natural dye-sensitized ZnO nano-particles as photo-catalysts in complete degradation of E. coli bacteria and their organic content," *Journal of Photochemistry and Photobiology A: Chemistry*, vol. 328, pp. 207-216, 2016.

[18] D. Chatterjee, S. Dasgupta, and N. N. Rao, "Visible light assisted photodegradation of halocarbons on the dye modified TiO_2 surface using visible light," *Solar Energy Materials and Solar Cells,* vol. 90, pp. 1013-1020, 2006.

[19] M. Aiempanakit, T. Tabtimsri, N. Triamnak, and C. Suwanchawalit, "Curcumin modified titanium dioxide nanotubes with enhanced visible light photocatalytic performance," *International Journal of Electrochemical Science*, vol. 14, pp. 1954-1967, 2019.

[20] M. Aiempanakit, J. Sangkaworn, N. Worawannotai, K. Laohhasurayotin, W. Sangchay, S. Lakseee, and C. Suwanchawalit, "Enhancement of Visible Light-Responsive Photocatalytic

Efficiency by Using a Laccaic Acid-Modified Titanium Dioxide Photocatalyst," *Journal of the Brazilian Chemical Society*, vol. 00, pp. 1-9, 2022.

[21] R. Rahimi, J. Shokraiyan, M. Rabbani, and F. Fayyaz, "Enhanced photobactericidal activity of ZnO nanorods modified by meso-tetrakis(4-sulfonatophenyl)porphyrin under visible LED lamp irradiation," *Water Science and Technology*, vol. 71, pp. 1249-1254, 2015.

[22] S. Radhika, and J. Thomas, "Solar light driven photocatalytic degradation of organic pollutants using ZnO nanorods coupled with photosensitive molecules," *Journal of Environmental Chemical Engineering*, vol. 5, pp. 4239-4250, 2017.

[23] X. Li, Y. Cheng, S. Kang, and J. Mu, "Preparation and enhanced visible light-driven catalytic activity of ZnO microrods sensitized by porphyrin heteroaggregate," *Applied Surface Science*, vol. 256, pp. 6705-6709, 2010.

[24] A. Haghighatzadeh, "Visible-light-active chlorophyll/flavonoid-sensitized ZnO nanoparticles: preparation and optical and photocatalytic studies," *Journal of the Australian Ceramic Society*, vol. 57, pp. 137-147, 2021.

[25] S. Landuma, D. A. Haryanto, and A. Purwanto, "Application of sappan wood (*Caesalpinia Sappan Linn*) as sensitizer for dye-sensitized solar cell (DSSC)," *AIP Conference Proceedings*, vol. 1586, pp. 109-112, 2014.

[26] P. Ohama, and N. Tumpat, "Textile dyeing with natural dye from sappan tree (*Caesalpinia sappan Linn.*) extract," *International Journal of Fashion and Textile Engineering*, vol. 8, pp. 432-434, 2014.

[27] T. E. Purbaningtias, I. D. Lestari, B. Wiyantoko, P. Kurniawati, and D. Sriadryani, "Utilization of natural indicators for borax identification in the Indonesian tofu," *AIP Conference Proceedings*, vol. 1823, p. 020057, 2017.

[28] A. Petdum, T. Sooksimuang, N. Wanichacheva, and J. Sirirak, "Natural colorimetric sensor from sappanwood for turn-on selective Fe^{2+} detection in aqueous media and its application in water and pharmaceutical samples," *Chemistry Letters*, vol. 48, pp. 678-681, 2019.

[29] N. P. Nirmal, M. S. Rajput, R. G. S. V. Prasad, and M. Ahmad, "Brazilin from *Caesalpinia sappan* heartwood and its pharmacological activities: A review," Asian Pacific Journal of Tropical Medicine, vol. 8, pp. 421-430, 2015.

[30] K. Mekala and R. Radha, "A review on sappan wood – A therapeutic dye yielding tree," *Research Journal of Pharmacognosy and Phytochemistry*, vol. 7, p. 227, 2015.

[31] C. Suwanchawalit, S. Wongnawa, P. Sriprang, and P. Meanha, "Enhancement of the photocatalytic performance of Ag-modified TiO_2 photocatalyst under visible light" *Ceramics International*, vol. 38, pp. 5201-5207, 2012.

[32] O. Mehraj, N. A. Mir, B. M. Pirzada, S. Sabir, and M. Muneer, "In-situ anion exchange synthesis of $AgBr/Ag_2CO_3$ hybrids with enhanced visible light photocatalytic activity and improved stability," *Journal of Molecular Catalysis A: Chemical*, vol. 395, pp. 16-24, 2014.

[33] H. Slimani, N. Bessous, S. Dagher, A. Hilal-Alnaqbi, M. El Gamal, B. Akhozheya, and M. Mohammed, "Growth of ZnO nanorods on FTO glass substrate," *Materials Research Express,* vol. 7, p. 025026, 2020.

[34] L. Ngamwonglumlert, S. Devahastin, N. Chiewchan, and G. S. Vijaya Raghavan "Color and molecular structure alterations of brazilein extracted from *Caesalpinia sappan* L. under different pH and heating conditions," *Scientific Reports*, vol. 10, p. 12386, 2020.

[35] J. Sirirak, N. Worawannotai, C. Suwanchawalit, and S. Chayabutra, "Preparation and characterization of lake pigments from sappan wood using Thai local clays," *Journal of Metals, Materials and Minerals*, vol. 30, no. 1, pp. 20-28, 2020.

[36] J. Sirirak, P. Suppharatthanya, K. Chantha, S. Girdthep, and S. Chayabutra, "Eco-friendly lake pigment from sappanwood: Adsorption study and its application as natural colorant for natural rubber toy balloon," *Journal of Metals, Materials and Minerals*, vol. 31, no. 2, pp. 27-37, 2021.

[37] G. Jiang, K. Geng, Y. Wu, Y. Han, and X. Shen, "High photocatalytic performance of ruthenium complexes sensitizing $g\text{-}C_3N_4/TiO_2$ hybrid in visible light irradiation," *Applied Catalysis B*, vol. 227, pp. 366-275. 2018.

[38] K. Parul, R. Kaur, P. Badru, P. Singh, and S. Kaushal, "Photodegradation of organic pollutants using heterojunctions: A review," *Journal of Environmental Chemical Engineering*, vol. 8, p. 103666, 2020.

[39] D. Chatterjee, S. Dasgupta, and N. N. Rao, "Visible light assisted photodegradation of halocarbons on the dye modified TiO_2 surface using visible light," *Solar Energy Materials and Solar Cells*, vol. 90, pp. 1013-1020, 2006.

[40] X. Zhang, Y. Wang, F. Hou, H. Li, Y. Yang, X. Zhang, Y. Yang, and Y. Wang, "Effects of Ag loading on structural and photocatalytic properties of flower-likeZnO microspheres," *Applied Surface Science*, vol. 391, pp. 476-483, 2017.

[41] T. Ganesh, J. H. Kim, S. J. Yoon, B. H. Kil, N. N. Maldar, J. W. Han, and S. H. Han, "Photoactive curcumin-derived dyes with surface anchoring moieties used in ZnO nanoparticle-based dye-sensitized solar cells," *Materials Chemistry and Physics*, vol. 123, pp. 62-66, 2010.

[42] S. Buddee, S. Wongnawa, P. Sriprang, and C. Sriwong, "Curcumin-sensitized TiO_2 for enhanced photodegrasation of dyes under visible light," *Journal of Nanoparticle Research*. vol. 16, p. 2336, 2014.

[43] M. A. Dil, A. Haghighatzadeh, and B. Mazinani, "Photosensitization effect on visible-light-induced photocatalytic performance of TiO_2/chlorophyll and flavoniod nanostructures: kinetic and isotherm studies," *Bulletin of Materials Science*, vol. 42, p. 248, 2019.